

Cite this: *Dalton Trans.*, 2021, **50**, 16739

# Precious metal complexes of bis(pyridyl)allenes: synthesis and catalytic and medicinal applications†

Hanna K. Maliszewska,<sup>a</sup> Carla Arnau del Valle,<sup>a</sup> Ying Xia,<sup>b</sup> María J. Marín,<sup>a</sup> Zoë A. E. Waller<sup>b,c</sup> and María Paz Muñoz<sup>\*a</sup>

The incorporation of donor-type substituents on the allene core opens up the possibility of coordination complexes in which the metal is bonded to the donor groups, with or without interaction with the double bond system. Despite the challenges in the synthesis of such allene-containing metal complexes, their unique 3D environments and dual functionality (allene and metal) could facilitate catalysis and interaction with chemical and biological systems. Bis(pyridyl)allenes are presented here as robust ligands for novel Pd(II), Pt(IV) and Au(III) complexes. Their synthesis, characterisation and first application as catalysts of benchmark reactions for Pd, Pt and Au are presented with interesting reactivity and selectivities. The complexes have also been probed as antimicrobial and anticancer agents with promising activities, and the first studies on their unusual interaction with several DNA structures will open new avenues for research in the area of metallodrugs with new mechanisms of action.

Received 31st August 2021,  
Accepted 28th October 2021

DOI: 10.1039/d1dt02929k

rsc.li/dalton

## Introduction

The development of ligand architectures with novel 3D arrangements is an important challenge in organic synthesis<sup>1–4</sup> with implications not only in the field of catalysis (and asymmetric catalysis), but also in the discovery of new organometallic complexes with potential for biological applications, currently an area of increasing growth.<sup>5–7</sup>

In this context, organic molecules displaying axial chirality, like biaryls or spiranes, have proven to be privileged structures in catalysis and have revolutionised the field of asymmetric catalysis.<sup>8–10</sup> However, despite progress in the field, it is still necessary to develop new chiral ligands to overcome limitations of established catalytic systems in terms of substrate scope, catalytic loading, turnover or enantioselectivity. Similarly, in medicinal organometallic chemistry, irrelevant to the metal studied, the rational design of the ligand seems crucial to control physical properties and selectivity towards specific biological targets. In many examples, stabilisation of a

metal complex is achieved by chelating the metal centre with multidentate ligands.<sup>11</sup>

In the context of novel ligand design, allenes<sup>12</sup> contain a backbone that goes beyond the tetrahedral chiral carbon or the chiral biaryl structures, creating a very attractive and unique 3D (axially chiral) environment that can be modulated and exploited in unprecedented applications.

Allene-containing natural products and synthetic molecules have been demonstrated to exhibit interesting biological activity, although little is known about their mode of action. Consequently, some efforts have been made in recent years to incorporate the allene moiety in the backbone of pharmacologically active compounds, including natural and non-natural products, to increase their interaction with biological targets, e.g. as enzymatic inhibitors.<sup>13</sup>

Besides, the use of organometallic and coordination metal complexes as drug candidates has some key advantages over classic organic compounds.<sup>14</sup> Recently, it has been reported that metal-containing compounds are statistically more likely to be active antimicrobial and antifungal agents than purely organic compounds (27% vs. 2% of compounds showing activity in each group, respectively).<sup>15</sup>

Moving away from the more documented class of  $\eta^2$  allene-metal complexes where the metal is solely bonded to one of the allene's double bonds (Fig. 1a),<sup>16–19</sup> the incorporation of donor-type substituents on the allene core opens the possibility of coordination complexes in which the metal is bonded to the donor groups, with or without interaction with the double bond system (LB = Lewis base, Fig. 1b).<sup>20–24</sup>

<sup>a</sup>School of Chemistry, University of East Anglia, Norwich Research Park, Norwich, NR4 7TJ, UK. E-mail: m.munoz-herranz@uea.ac.uk

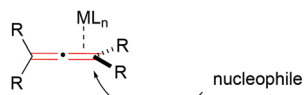
<sup>b</sup>School of Pharmacy, University of East Anglia, Norwich Research Park, Norwich, NR4 7TJ, UK

<sup>c</sup>UCL School of Pharmacy, 29-39 Brunswick Square, London, WC1N 1AX, UK

† Electronic supplementary information (ESI) available: Synthesis and characterisation of ligands and metal complexes, catalytic and electrochemical experiments, spectral data, X-ray details for complex **2b**, experiments of stability of **3a–b** in solution, experimental details of the antimicrobial, anticancer and interaction with DNA studies. CCDC 2094617. For ESI and crystallographic data in CIF or other electronic format see DOI: 10.1039/d1dt02929k



## a) Classic allene-metal coordination.



## b) Allene as novel ligand architecture. This work.

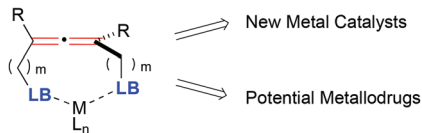


Fig. 1 Different types of interaction of allene frameworks with metals.

Creation of such allene containing-metal complexes presents significant synthetic challenges, *e.g.* competing coordination of the metal to the double bond and the donor atoms, and the control of nucleophilic attack of one donor atom to the allene activated by the metal that would destroy the allene backbone. Despite these inherent challenges, this design offers many advantages: the unique stereochemistry of the allene backbone creates novel 3D environments that could facilitate catalysis and asymmetric induction in chemical and biological systems; the multiple sites of coordination could increase the stability of the new metal species; and the presence of the metal in close proximity to the allene core can potentially activate the allene as a Michael acceptor to react with nucleophilic residues of enzymes, proteins or nucleic acids, giving these new metalloodrugs alternative and/or synergistic modes of action, unique from current organometallic drug molecules. These characteristics could be key to the development of new catalysts and drugs. Therefore, allene-containing metal complexes have the potential to be exploited for their unique 3D shapes for studies in both catalytic and medicinal settings.

Despite some initial promising results using allene-containing phosphines as ligands in Rh(I) (Fig. 2a) and Au(I) (Fig. 2b,

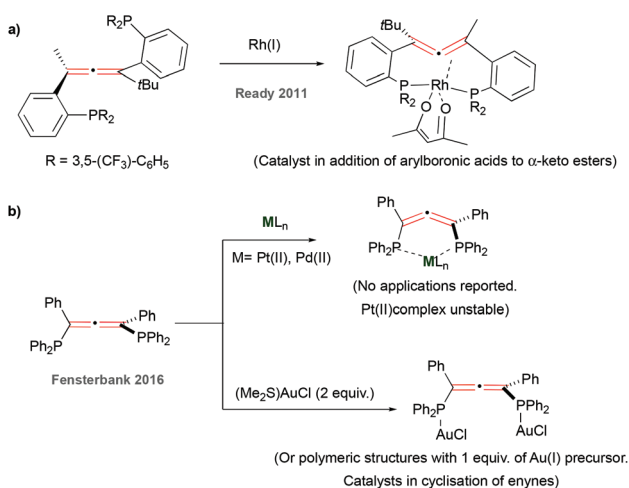


Fig. 2 Previous work with allene-containing phosphines as ligands.

bottom) catalysis, reported by Ready<sup>23</sup> and Fensterbank<sup>24</sup> respectively, the Pd(II) and Pt(II) complexes of phosphine containing ligands (Fig. 2b, top)<sup>24</sup> have not been reported in any catalytic applications. Since these seminal works, there have not been further developments in the field, possibly due to the rapid oxidation of these systems when exposed to air.<sup>25</sup> Specifically, this makes phosphine analogues less attractive to use as ligands for complexes to be used in biological applications.<sup>20,21,26</sup>

In contrast, N-containing ligands such as bi- and ter-pyridines, have been widely used for the stabilisation of metal complexes by at least two chelating nitrogen donors, which lowers the reduction potential of the metal centre, making them more stable under physiological conditions.<sup>11</sup> This makes pyridyl groups stand out as especially attractive structures to incorporate in the allene ligand design.

In 2008, Krause and co-workers prepared bis(pyridyl)allene ligands and postulated the formation of their Cu(I) and Ag(I) complexes (Fig. 3a, top). However, not all the metallic structures were fully characterised and their use in any applications has not been reported since.<sup>22</sup> Later on, Fensterbank and co-workers observed that pyridyl-containing phosphine oxide (allenes) underwent nucleophilic intramolecular attack of the pyridine onto the allene to form cyclic metal species in the presence of Au(I) (Fig. 3a, bottom).<sup>27</sup> The difficulty in isolation and characterisation of pyridyl-based allene-containing metal complexes was further underpinned by our investigation into Au(I) and Au(III) coordination chemistry of bis(pyridyl)allenes, that also underwent cyclisation in the presence of these metal centres (Fig. 3a, bottom).<sup>28</sup>

To date applications of bis(pyridyl)allene-based metal systems remain totally unexplored, not only in the area of catalysis, but also in their use in a biological context. This latter application has also been completely uncharted in reported phosphine analogues, which gives this work additional signifi-

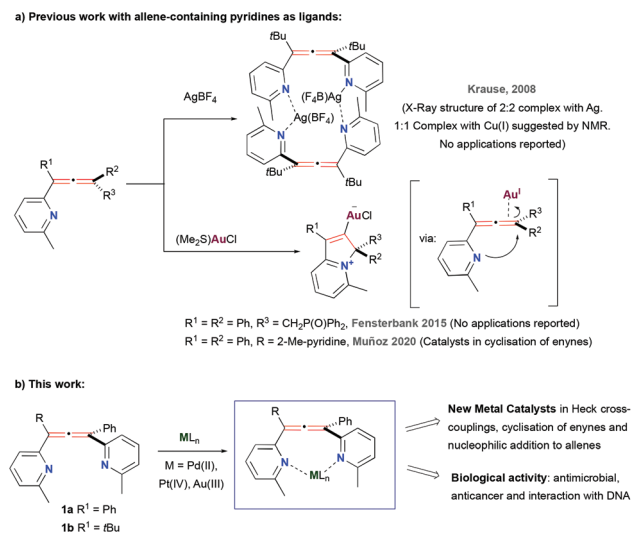


Fig. 3 Previous (a) and present (b) work with allene-containing pyridines as ligands.



cance. The many benefits and unexplored applications of these systems prompted us to explore their synthesis further. Here, we report the synthesis and characterisation of Pd(II), Pt(IV) and Au(III) bis(pyridyl)allene-containing complexes, and the explorative exploitation of their unique structures as catalysts and as potential metallodrugs in three settings, as antimicrobial agents, as anticancer drugs and their specific interaction with different structures of DNA. The preliminary data reported here will be crucial for further development of the complexes with applications in both areas (Fig. 3b, this work).

## Results and discussion

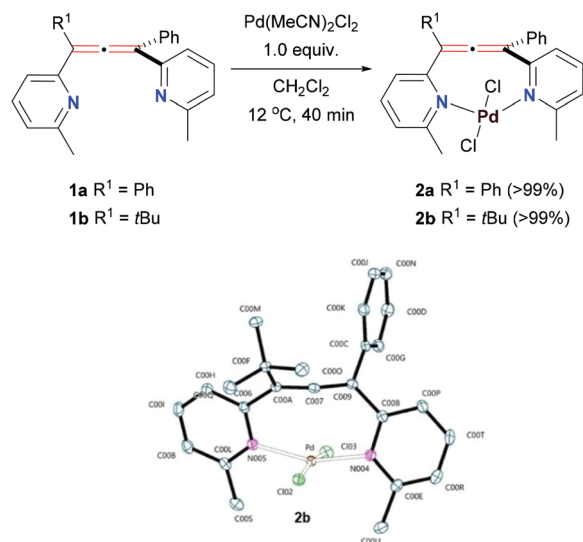
### Synthesis of bis(pyridyl)allene metal complexes

We achieved the racemic synthesis of bis(pyridyl)allene ligands **1a–b** (Fig. 3b) according to modified literature procedures (see ESI,† section 2.1). These compounds are stable in solution (in chlorinated solvents, alcohols, DMSO, MeCN) and solid state, at room and elevated temperature, and under air, which highlights their robustness as promising ligands.

With the ligands in hand, we proceeded to expand the coordination properties of bis(pyridyl)allenes beyond the reported Cu(I) and Ag(I) complexes. The choice of metals for the complexation studies was two-fold. On the one hand, Pd, Pt and Au are versatile metals in important catalytic processes, so there is ample data to compare with the state-of-the-art metal complexes in those transformations.<sup>29–32</sup> On the other hand, Pt and Au are one of the most common metals used in medicine,<sup>33–35</sup> and although Pd has been much less explored, there is emerging data that shows it might have good potential in interaction with biological systems.<sup>36</sup>

Starting with Pd(II) precursors, the ligands were reacted with 1 equiv. of Pd(MeCN)<sub>2</sub>Cl<sub>2</sub> in dichloromethane. The reaction mixture changed colour from yellow to red over the course of 40 min, giving quantitative formation of new metal species (**2a–b**, Scheme 1, top).

<sup>1</sup>H and <sup>13</sup>C NMR analyses of **2a** revealed that the symmetry of the ligand was maintained in the complex, but the corresponding peaks were shifted. For instance, the methyl peak on the <sup>1</sup>H NMR spectrum moved from 2.58 ppm in **1a** to 3.17 ppm in **2a**, while the peak corresponding to the central allene carbon atom shifted up-field from 212.7 ppm to 204.1 ppm, respectively ( $\Delta\delta = 8.6$  ppm, see ESI,† section 2.2). These observations led us to propose the bidentate structure of **2a**, where Pd is captured by both pyridyl units and sits in the pocket created by the frame of the ligand, with the allene group itself not engaged in bonding to the metal centre. HRMS and EA analysis provided further evidence supporting the structure with 1:1 ligand to metal stoichiometry. Additionally, we obtained good quality crystals of the non-symmetric complex **2b**, and its structure was unambiguously confirmed by X-ray crystallography (Scheme 1, bottom). The structure **2b** clearly shows the undisturbed allene unit with the C(A)–C(7)–C(9) angle measured at 172.3°. Similarly, the typical double bond distances of the allene found at 1.321(2) Å and

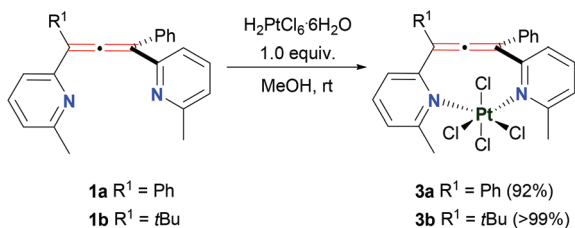


**Scheme 1** Synthesis of Pd(II)-complexes **2a–b** and ORTEP representation of the X-ray of complex **2b** (Hs omitted).

1.322(2) Å are indicative of a non-metal bonded allene group. The long distance of the Pd centre to the central carbon of the allene, 2.5038 (1) Å, confirms the Pd centre is not bonding to the central carbon of the allene. As we expected, the nitrogen atoms of both pyridines are facing inwards the ligand's pocket and are engaged in bonding to the Pd, with bond lengths of Pd–N(5) 2.0489(1) Å and Pd–N(4) 2.0269(1) Å. Overall, the perpendicular arrangement of the allene ligand is maintained and Pd is enclosed within. Complex **2b** features very slightly distorted square planar geometry typical for Pd(II) complexes. The coordination sphere is completed by two chloride ligands equally distanced from the metal centre (2.3300(4) Å and 2.3203(5) Å). Interestingly, **2b** is bonded to Pd in a *trans* arrangement. There are only few examples of such bidentate, *trans*-spanning ligands based on pyridyl groups reported to date.<sup>37,38</sup> Formation of *trans* isomers of complexes with these ligands might have beneficial consequences for their use in catalysis. For example, *trans*-spanning pyridyl ligands have been observed to be more active catalysts in Heck coupling reaction.<sup>39</sup> We could not obtain good enough crystals of the symmetric **2a** to perform the crystallographic analysis, so full assignment of the geometry (*cis* or *trans*) could not be confirmed. Although we initially assumed *trans* geometry of **2a**, based on the similarity of the remaining characterisation data, the differences in catalytic behaviour of both complexes in the Pd-catalysed cross-coupling reactions (*vide infra*) would suggest that **2a** could be predominantly *cis*.<sup>40</sup>

Interestingly, **1a–b** were completely unreactive towards Pt(II) salts when we tried to access the Pt(II) analogues of **2a–b** in a similar manner. Reactions with a variety of Pt precursors (PtCl<sub>2</sub>, Pt(MeCN)<sub>2</sub>Cl<sub>2</sub>, K<sub>2</sub>PtCl<sub>4</sub>, *cis*-Pt(DMSO)<sub>2</sub>Cl<sub>2</sub>, *etc.*) under a range of conditions (*e.g.* solvents and temperature, see ESI,† section 2.2) usually resulted in the recovery of unreacted starting materials. We considered that the reaction with a smaller



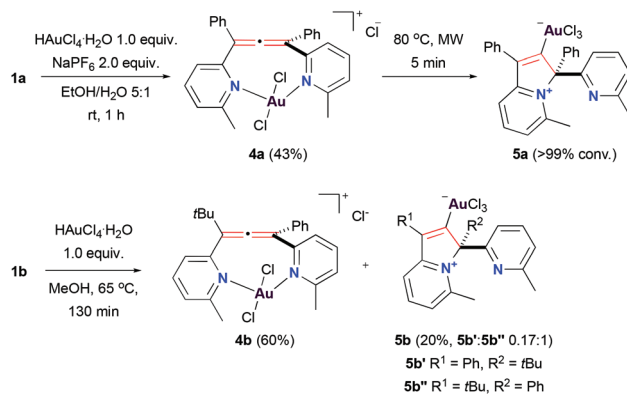


Scheme 2 Synthesis of Pt(IV)-complexes 3a–b.

Pt(IV) centre might be more feasible.<sup>41</sup> To test this, we reacted ligands **1a–b** with 1 equiv. of chloroplatinic(IV) acid (Scheme 2). We were happy to observe the immediate formation of orange powder products in both cases. These powders were the new Pt(IV) complexes **3a–b** with 1 : 1 ligand to metal stoichiometry, confirmed by <sup>1</sup>H and <sup>13</sup>C NMR, HRMS and EA analyses (see ESI,† section 2.2). Noteworthy, the NMR spectra of **3a** were still characterised by an increased symmetry indicative of a bidentate nature of the ligand. The data also suggested that the allene core did not participate in the metal complexation. Both complexes **3a–b** were only soluble in DMSO, with **3a** not being very stable in solution over long periods of time (see ESI,† section 5), which made obtaining good crystals for X-ray analysis difficult. In these cases, we proposed an octahedral geometry of the metal centre typical for Pt(IV) complexes and draw the structures as *cis* isomers. The *trans* isomer would require one of the chloride ligands to be placed directly in the space between the Pt atom and the centre of the allene or the distortion of the octahedral geometry. Although, the NMR data indicated that the allene environment did not substantially change in **3a–b** compared to the free ligands, we cannot completely rule out either isomer. In fact, the broadening of signals observed on the NMR spectra could be a reflection of the equilibrium between the *cis* and *trans* isomers in solution.<sup>42</sup>

The synthesis of the novel Pt(IV) bis(pyridyl)allene complexes brings a two-fold advantage. First of all, Pt(IV) complexes have been extensively studied as pro-drugs for anticancer therapy.<sup>43–45</sup> Pt(IV) compounds are considered as potential precursors to the active Pt(II) species and are designed to circumvent some of the undesired side effects of the latter. Hence, the cytotoxicity and redox chemistry of **3a–b** would be of much interest. Secondly, Pt(IV) compounds can be used as synthetic precursors to more challenging Pt(II) equivalents by means of chemical or electrochemical reduction. Unfortunately, our attempts to access direct Pt(II) analogues of **3a–b** *via* chemical reduction were unsuccessful (see ESI,† section 2.2). The more reactive **3b** underwent cycloplatination under reducing conditions losing the allene core in the process.<sup>28</sup> Inertness of **3a–b** under milder reduction conditions might be explained by their quite negative Pt(IV)/Pt(II) reduction potentials found at –1.0 V and –1.1 V, respectively for **3a** and **3b**, as measured by cyclic voltammetry of these complexes (see ESI,† section 2.2).

We explored the chemistry of bis(pyridyl)allenes with Au next. We previously reported that in the presence of Au(I)



Scheme 3 Synthesis of Au(III)-complexes 4a–b and 5a–b.

sources these ligands undergo cyclisation triggered by activation of the allene unit by the carbophilic Au(I) and attack of the pyridyl group onto the terminal carbon of the allene.<sup>28</sup> However, the different nature of the Au(III) centre allowed the access to unprecedented Au(III) complexes with the allene moiety intact (Scheme 3).

In this case, each of the ligands required slightly different reaction conditions to facilitate the formation of the allene-containing complex. Thus, **1a** reacted with 1 equiv. of chloroauric(III) acid in a mixture of ethanol and water at room temperature to give Au(III) complex **4a** in 43% yield. Attempts to improve the efficiency of the reaction, for example, by increasing the temperature, resulted in full conversion into the cyclic product **5a**, observed in our previous work.<sup>28</sup> On the other hand, reaction of **1b** in refluxing methanol yielded a mixture of allene-containing complex **4b** and mixture of isomers of the cyclised **5b** that could be easily separated afterwards, as previously reported.<sup>28</sup> Characterisation of **4a–b** confirmed the presence of the allene moiety and the *N,N*-chelating character of these complexes. Complexes **4a–b** are drawn as *trans* isomers in analogy to the square planar Pd(II) examples due to the similarities on the <sup>13</sup>C NMR shifts on the central carbon of the allene (see ESI,† section 2.2).

### Catalytic applications

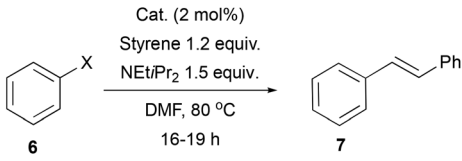
To explore the utility of our compounds as catalysts, we chose several benchmark reactions used in the evaluation of new catalysts depending on the metal used. We only tested the complexes in their racemic version, but success on this area will open avenues of research in the asymmetric variants (due to the axial chirality of the allene framework), making them worth exploring as catalysts.

### Mizoroki–Heck cross-coupling

We began testing the Pd compounds **2a–b** in the Mizoroki–Heck cross-coupling reaction (Table 1).<sup>46–48</sup> A standard coupling between styrene and aryl halides (**6**, PhX, X = I or Br) was performed with 2 mol% catalyst loading. We observed formation of (*E*)-stilbene **7** in reaction with iodobenzene catalysed





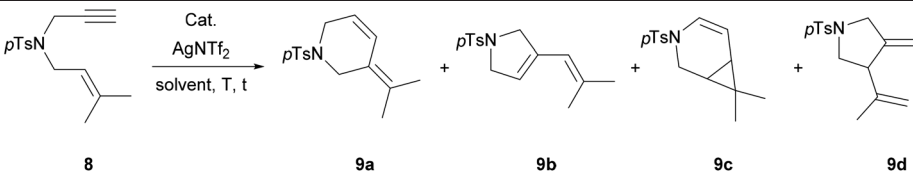
**Table 1** Catalytic activity of Pd(II)-complexes **2a–b** in Mizoroki–Heck couplings


Entry	Cat.	X	Additives	Yield (%)
1	<b>2a</b>	I	HCO <sub>2</sub> NH <sub>4</sub> (10 mol%)	87
2	<b>2a</b>	I	—	93
3	<b>2a</b>	Br	—	20
4	<b>2b</b>	I	—	36
5	<b>2b</b>	Br	—	—

by **2a**. The use of additives, such as HCO<sub>2</sub>NH<sub>4</sub>, was not necessary to obtain an excellent yield of the product (Table 1, entry 1 vs. entry 2). The activity of **2a** was substantially diminished in a reaction with bromobenzene (Table 1, entry 3). Non-symmetric complex **2b** was less active, giving a moderate yield in the reaction with PhI (36% yield, Table 1, entry 4) and showing no activity in the coupling with PhBr (Table 1, entry 5). The difference in activity between the two catalysts could be attributed, for example, to the steric bulk near the catalytic centre in **2b**, e.g. the access of starting materials might be more hindered for the *t*-butyl substituted complex. We could also explain the discrepancy if we consider complex **2a** to be in fact predominantly *cis* rather than *trans* like **2b**. Although further tuning of the catalyst design is needed to increase the activity with more challenging substrates, we present here the first example of an allene-derived catalytic system used in such an important process that could open further research and developments also in the asymmetric version.

### Cyclisation of enynes

The catalytic activity of all complexes was next evaluated in reactions of 1,6-enynes (Table 2 and ESI,† sections 2.4 and 2.5).<sup>30,49–52</sup> We observed an initial lack of activity of Pd(II) and Pt(IV) compounds in the absence of AgNTf<sub>2</sub>, either at room temperature or at 80 °C (Table 2, entries 1–4). These observations were consistent with a known heightened reactivity of cationic complexes in the catalysis involving enynes.<sup>53,54</sup> Thus, to ensure the formation of the cationic catalytic species and improve the activity, the synthesised catalysts were subsequently used in the presence of excess AgNTf<sub>2</sub> in toluene at 80 °C (Table 2, entries 5–8). One-hour long reactions with all the Pd(II) and Pt(IV) catalysts resulted in excellent conversions and yields. Interestingly, a switch between catalysts based on different metal centres allowed to achieve selectivity towards different isomeric products. Pd-Complexes **2a–b** favoured formation of a cyclopropane bicycle **9c**, while Pt-ones **3a–b** gave 6-membered skeletal rearrangement **9a** and Alder–ene **9d** as major reaction products. We restricted the use of Au(III) allene-containing complexes **4a–b** to a near room temperature conditions to avoid the cyclisation to carbene species during the catalytic reaction. Although these complexes showed to be active even without addition of AgNTf<sub>2</sub> providing further evidence of their cationic character (see ESI,† section 2.4), they were tested with the addition of AgNTf<sub>2</sub> here to boost the reactivity at room temperature (Table 2, entries 9 and 10). We observed only moderate conversions after 1.5 h, although this time the major product of the reaction was the 5-membered skeletal rearrangement product **9b**. Furthermore, Pt-complexes **3a–b** performed well as catalysts in the alkoxy-cyclisation of all enynes tested, when the reaction was carried out in MeOH. Interestingly, when *N*-tethered enynes (**8**) were investigated, Au-complexes **4a–b** seemed to give better results (see ESI,† section 2.5).<sup>55–57</sup>

**Table 2** Catalytic activity of complexes **2a–b**, **3a–b** and **4a–b** in cyclisation of enynes


Entry	Cat. (mol%)	[AgNTf <sub>2</sub> ] (mol%)	Solvent	T (°C)	t (h)	8	9a	9b	9c	9d	Conv. (%)	Yield (%)
1	<b>2a</b> (3)	—	CH <sub>2</sub> Cl <sub>2</sub>	rt	1.5	1.0	—	—	—	—	0	—
2	<b>3a</b> (3)	—	CH <sub>2</sub> Cl <sub>2</sub>	rt	1.5	1.0	—	—	—	—	0	—
3	<b>2a</b> (3)	— <sup>a</sup>	PhMe	80	1	1.0	—	—	—	—	n. is. <sup>b</sup>	n. is. <sup>b</sup>
4	<b>3a</b> (3)	—	PhMe	80	16	1.0	—	—	—	—	0	—
5	<b>2a</b> (3)	6.5	PhMe	80	1	—	0.6	—	1.0	0.06	>99	>99
6	<b>2b</b> (3)	6.5	PhMe	80	1	0.08	0.4	—	1.0	0.07	95	85
7	<b>3a</b> (3)	6.5	PhMe	80	1	—	0.8	0.3	0.4	1.0 <sup>c</sup>	>99	88
8	<b>3b</b> (3)	6.5	PhMe	80	1	—	1.0	0.35	0.4	1.0 <sup>c</sup>	>99	>99
9	<b>4a</b> (2)	2.5	CH <sub>2</sub> Cl <sub>2</sub>	rt	1.5	1.0	0.14	0.4	0.05	—	37	36
10	<b>4b</b> (2)	2.5	CH <sub>2</sub> Cl <sub>2</sub>	rt	1.5	1.0	0.08	0.25	0.03	—	26	26

<sup>a</sup> [Ag]<sup>+</sup> added after 1 h. <sup>b</sup> n. is. = not isolated. <sup>c</sup> Unidentified product also obtained (0.35 ratio).



### Nucleophilic addition to allenes

To further test the robustness as catalysts of our new allene-derived complexes, we thought it would be an interesting challenge to use them in reactions involving allenes, like the well-explored metal-catalysed nucleophilic addition to allenes.<sup>58,59</sup>

For this, we chose, as model, the reaction between allene-phthalimide **10** and benzyl alcohol. The Pt(IV)-complexes **3a–b** were the most active catalysts from the group (Table 3, entries 1 and 2). Both resulted in complete conversions and formation of the distal double addition product – acetal **11a** corresponding to the usual reactivity with Pt(II) catalysts.<sup>60–63</sup> Acetal **11a** was also isolated in its hydrolysed form of the aldehyde **12a**. Interestingly, a minor product of the reaction (**11b**) was identified as the double addition product to the central carbon atom of the allene that readily hydrolysed to ketone **12b** upon handling. This type of reactivity has been previously observed only with thiol nucleophiles under Au(III) catalysis.<sup>64</sup> However, our Au(III)-complex **4b** promoted the formation of the single distal addition alkene product **13**, albeit with low conversion (Table 3, entry 3), showing reactivity typical for Au(I) catalysis.<sup>65,66</sup> Pd(II)-Complex **2a** however, was unreactive under the reaction conditions (Table 3, entry 4).

Although the Au(III) and Pd(II) complexes yielded low reactivity, the Pt(IV) ones gave results in line with state-of-the-art reactivity of Pt complexes with the advantage of working at room temperature and being the first examples in which an allene-containing Pt catalyst is used to catalyse a reaction involving allene compounds.<sup>67</sup>

### Bioactivity

In a more novel application, we explored the unique 3D geometries of the new organometallics containing allenes, as potential metallodrugs in three settings: as antimicrobial agents (in collaboration with Community for Open Antimicrobial Drug Discovery – CO-ADD), as anticancer drugs and their specific interaction with different structures of DNA (double helical, i-motif and G-quadruplex). Promising results in these areas will

open future studies on the mechanism of action, speciation and the nature of the bioactive species in each of the biological settings, which are out of the scope of this work.

### Antimicrobial studies

Complexes **2–4** and ligands **1a–b** were tested for their antimicrobial activity in collaboration with the Community for Open Antimicrobial Drug Discovery (CO-ADD).<sup>68</sup> The initial screening against microorganisms from Gram-negative bacteria (G –ve), Gram-positive bacteria (G +ve) and fungi groups at single drug concentration of 32  $\mu\text{g mL}^{-1}$  (see ESI,† section 6) showed that all complexes were active (percentage of microorganism growth inhibition >80%) against at least one of the groups of microorganisms at that concentration, with the exception of complex **3a**, that was completely inactive. The ligands **1a–b** alone did not show any activity when tested at the same concentration against the same microorganisms.

Dose–response studies (in the concentration range of 0.25–32  $\mu\text{g mL}^{-1}$ ) of these complexes (except **3a**) were performed with the same microorganism species to determine the minimum inhibitory concentration (MIC) value.<sup>69</sup> The activity of complexes **2** and **4** was confirmed against a selection of the microorganisms, a G +ve bacteria, *Staphylococcus aureus* (*S. aureus*), and two yeasts, *Candida albicans* (*C. albicans*) and *Cryptococcus neoformans* (*C. neoformans*) var. *grubii* (Table 4, entries 1, 2 and 4, 5), with complex **2b** being the most active one, showing remarkably low MIC values of  $\leq 0.25 \mu\text{g mL}^{-1}$  (Table 4, entry 2).<sup>70,71</sup> Although complex **3b** exhibited activity in the single dose assay, it showed no induction of growth inhibition at lower concentrations with any of the microorganisms tested (Table 4, entry 3).

Additionally, cytotoxicity of the new complexes was probed against human embryonic kidney cells (HEK-293) as the standard model for human cells used by the CO-ADD (Table 4). Cytotoxicity was expressed as a  $\text{CC}_{50}$  value – concentration at 50% cytotoxicity. The compounds with  $\text{CC}_{50}$  equal or lower than the maximum tested concentration (32  $\mu\text{g mL}^{-1}$ ) were

**Table 3** Catalytic activity of complexes **2–4** in the nucleophilic addition of benzyl alcohol to allene-phthalimide **10**

Entry	Cat.	AgNTf <sub>2</sub> (mol%)	t (h)	<b>10</b>	<b>11a</b>	<b>12a</b>	<b>11b/12b</b>	<b>13</b>	Conv. (%)
1	<b>3a</b>	10	26	—	1.0	0.4	0.08	—	>99 <sup>a</sup>
2	<b>3b</b>	10	27	—	1.0	0.24	0.07	—	>99 <sup>b</sup>
3	<b>4b</b>	5	27	1.0	—	—	—	0.2	17
4	<b>2a</b>	10	24	1.0	—	—	—	—	0

<sup>a</sup> Isolated yield 67%. <sup>b</sup> Isolated yield 61%.



**Table 4** Minimum inhibitory concentration (MIC,  $\mu\text{g mL}^{-1}$ ) on selected microorganisms, in a range of 0.25–32  $\mu\text{g mL}^{-1}$  of the drug (complexes 2–4) concentration; CC<sub>50</sub> (cytotoxicity,  $\mu\text{g mL}^{-1}$ ) with HEK-293 cells; HC<sub>10</sub> (haemolytic activity,  $\mu\text{g mL}^{-1}$ ) with RBC cells

Entry	Complex	G +ve MIC [ $\mu\text{g mL}^{-1}$ ] <i>S. aureus</i>	Yeast		Human	
			<i>C. albicans</i>	<i>C. neoformans var. grubii</i>	CC <sub>50</sub> [ $\mu\text{g mL}^{-1}$ ] Embryonic kidney cells HEK-293	HC <sub>10</sub> [ $\mu\text{g mL}^{-1}$ ] Red blood cells RBC
1	<b>2a</b>	2	16	1	0.9567	>32
2	<b>2b</b>	≤0.25	≤0.25	≤0.25	1.066	>32
3	<b>3b</b>	>32	32	>32	>32	>32
4	<b>4a</b>	16	4	16	>32	>32
5	<b>4b</b>	16	4	≤0.25	>32	≤0.25

considered toxic. This included the most promising active Pd(II)-complex **2b** and the analogous **2a** that also showed good activity in the dose–response assay.

Au(III)-complexes **4a** and **4b** were moderately active against the microorganisms. However, **4b** showed haemolytic activity against human red blood cells (RBC),<sup>72</sup> which prevented further *in vivo* testing (using moth larvae *Galleria mellonella*).

Although complex **4a** seemed to be the most promising lead for antibiotic activity and non-toxic to selected human cells, the activity was moderate compared with current organometallics leads<sup>15,73–76</sup> and it was not selected for *in vivo* studies. However, these preliminary results, open the door for further studies with analogues of Au(III)-complexes **4** as promising novel antimicrobial drugs.<sup>77–79</sup>

### Anticancer studies

In parallel to the antimicrobial studies, we investigated the preliminary *in vitro* anticancer activity of the new library of compounds 2–4 against the human breast adenocarcinoma cell line MDA-MB-231 (see ESI,† section 7), a triple-negative breast cancer cell line difficult to treat with current therapies and causing poorer outcomes for patients in comparison with other subtypes.<sup>80</sup>

The initial experiments were carried out with a concentration range of 0.19–100  $\mu\text{M}$  over a 24 h incubation period, using the CellTiter-Blue assay to measure cell viability. Interestingly, only symmetric complexes of Pd(II) **2a** and Au(III) **4a** showed effects on MDA-MB-231 cell viability in the low micromolar range, while **2b** and **4b** were significantly less active. In particular, **2b** showed no activity even at the highest concentration tested (100  $\mu\text{M}$ ). Pt(IV) complexes **3a–b** did not show a clear sigmoidal trend of diminished cell survival, which could be attributed to solubility issues in the aqueous media, difficulties in the uptake into the cells or thwarted reduction to more active Pt(II) species, as we experienced in the chemical and electrochemical reduction experiments described above.

The free ligands **1a–b** did not show any effect on cell survival in line with the results seen in the antimicrobial activity studies (*vide supra*).

We validated the results of the more promising complexes **2a** and **4a** using the MTT assay, which measures cell metabolic activity, in a similar concentration range with a 24 h incu-

bation period. The IC<sub>50</sub> values for complexes **2a** and **4a** were determined to be  $3.32 \pm 1.22$  and  $2.50 \pm 1.63$   $\mu\text{M}$ , using the MTT assay. These values are within the range obtained for reported Pd(II) (IC<sub>50</sub> ca. 0.5–22.9  $\mu\text{M}$ )<sup>81–85</sup> and Au(III) (IC<sub>50</sub> ca. 0.3–11.2  $\mu\text{M}$ )<sup>86,87</sup> complexes, and lower than reported values for cisplatin (IC<sub>50</sub> ca. 25–50  $\mu\text{M}$  depending on the study) against the MDA-MB-231 cell line. These results highlight the potential of our 3D metal complexes as new scaffolds for anti-cancer drug discovery.

As mentioned before, preliminary cytotoxicity results on embryonic kidney cells and red blood human cells were carried out as part of the antimicrobial study by our collaborators at CO-ADD (*vide supra*, Table 4). Neither complex showed haemolytic activity against human red blood cells. Although complex **2a** showed cytotoxicity towards embryonic kidney cells, complex **4a** did not, which could support further testing of this complex and new analogues, extending the study to other cancer cell lines and biocompatibility studies towards healthy human breast tissue.

### DNA studies

The mechanism of action of many metal-based drugs is often, at least partially, ascribed to their interactions with DNA as an intracellular target (*e.g.* cisplatin, oxaliplatin, carboplatin).<sup>88–92</sup> We wanted to probe the possible source of the activity of the allene-containing metal complexes in anticancer assays by studying their interactions with different DNA types, not only with the standard double stranded helical structure, but also with non-canonical DNA secondary structures – such as G-quadruplexes and i-motifs.<sup>93</sup> These sequences are widespread throughout the human genome and can be found in promoter regions of their genes (for example the gene encoding death associated protein, DAP)<sup>94</sup> and in the telomeres.<sup>95</sup> In particular, the telomeric region of DNA and associated proteins have been linked to important functions such as DNA replication and protection against DNA damage.<sup>96</sup> As such, the link between dysfunctional telomeric DNA and disease *e.g.* cancer, is of much interest.<sup>97</sup>

The screening of the new complexes 2–4 and the free ligands **1a–b** was performed with several types of DNA: double helical DNA (DS), the i-motif (hTeloC) and G-quadruplex (hTeloG) structures from the human telomere and i-motif forming sequences from the promoter regions of hif-1- $\alpha$  and



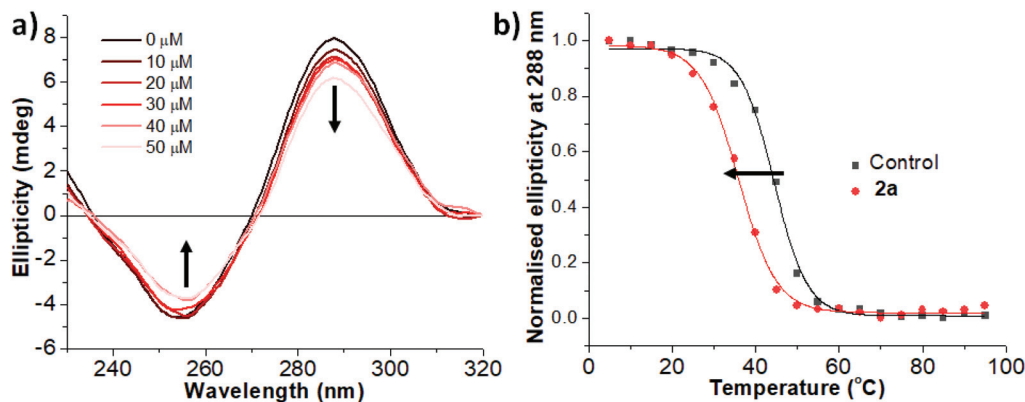


Fig. 4 Interaction of compound **2a** with i-motif DNA. (a) Circular dichroism spectroscopy of hTeloC (10  $\mu$ M) in 10 mM sodium cacodylate buffer, 100 mM KCl, pH 5.5. 0–5 equiv. of compound **2a**. (b) CD melting experiment with hTeloC in the absence (black) and in the presence of 5 equiv. of compound **2a** (red).

DAP,<sup>98</sup> using fluorescence intercalator displacement (FID) assays with thiazole orange (TO) as the fluorescent probe (see ESI,<sup>†</sup> section 8.2).<sup>99</sup> The compounds were tested at a single concentration (2.5  $\mu$ M, 5 equiv. in respect to DNA). In these assays, the ligands **1a–b** did not show displacement of the TO probe with any of the DNA structures, in line with the lack of activity observed in the antimicrobial and anticancer assays. This result provides further evidence that any observed bioactivity of the allene-derived metal complexes is probably not linked to the action of disassociated ligands if such de-complexation would take place under physiological conditions.

In contrast, Pd(II)-complexes **2a** and **2b** exhibited displacement of TO from hTeloG, showing partial affinity for the G-quadruplex sequence (35% and 48% for **2a** and **2b** respectively). These two Pd complexes were also the most active binders for all i-motif sequences, reaching displacement levels of 87% for **2b** with hTeloC.

Pt(IV) complexes **3a–b** were inactive on the level of the free allene ligands **1a–b**, and both Au(III)-complexes **4a–b** interacted with the DNA to a much lesser extent.<sup>100</sup> This would be in agreement with the mode of action of other Au(III) complexes, that are reported to be more prone to interact with protein targets.<sup>101–106</sup>

The more promising binders, Pd complexes **2a–b**, were further examined using circular dichroism (CD) spectroscopy (**2a**, Fig. 4).<sup>107</sup> By virtue of the significant number of studies of G-quadruplex binding compounds, there are a few examples of Pd complexes interacting with G-quadruplex DNA.<sup>108–110</sup> However, to the best of our knowledge, there are no studies that have looked at Pd complexes and their interaction with i-motif DNA.<sup>111</sup>

Pd-Complex **2a** was first titrated against hTeloC up to 5 : 1 ligand to DNA ratio (Fig. 4a).<sup>112</sup> The characteristic i-motif peaks were observed at around 255 nm (negative) and 288 nm (positive). The increasing excess of **2a** induced a visible hypochromic shift of both peaks, that is usually associated with an unfolding effect of the DNA secondary structure. CD-melting experiments were performed to quantify the effects on the

stability of the DNA structures. A plot of normalised ellipticity vs. temperature for the peak at 288 nm allowed to find the values of the melting temperature for the hTeloC sequence with (red circle) and without (black square) the Pd complexes (Fig. 4b), and hence the change in melting temperature ( $\Delta T_m$ ) value of  $-8.1 \pm 0.8$  °C, which indicates destabilisation of this i-motif DNA structure in the presence of the complex. This is similar in potency to the destabilisation of i-motif caused by commonly-used G-quadruplex stabilising ligands.<sup>113,114</sup> Complex **2b** also showed a change in melting temperature ( $\Delta T_m = -2.1 \pm 0.1$  °C) for hTeloC, albeit smaller than that for **2a**. Although there are many types of ligands capable of interacting with G-quadruplex DNA, compounds that interact with i-motif are very rare. Importantly these complexes did not significantly alter the stability of any other DNA structure examined, indicating some specificity for destabilising the i-motif form hTeloC. These unusual properties of our allene-containing Pd(II)-complexes and their different interaction with DNA structures, provide further indication of the promise of these new chemical scaffolds as leads for future medicinal applications.

## Conclusions

In summary, we present here bis(pyridyl)allenes as robust ligands for novel Pd(II), Pt(IV) and Au(III) complexes with unique 3D architectures for application in two important areas, catalysis and medicinal chemistry. While Pd(II) and Pt(IV) complexes were easily obtained, the isolation of Au(III) complexes needed careful control of the reaction conditions to avoid cyclisation of the ligand framework to form Au(III) carbene derivatives. Crystal structure analysis of the Pd(II) complex **2b** showed an unusual *trans* geometry. The Pt(IV) complexes **3a–b** seemed to display octahedral geometry and *cis-trans* ligand isomerisation in solution. Electrochemical analysis showed quite negative Pt(IV)/Pt(II) reduction potentials, and cycloplatination occurred with **3b** when forcing chemical





reduction conditions were applied. The analogue Au(III) complexes **4a–b** containing intact allenes as ligands were isolated when the reaction of the ligands **1a–b** and Au(III) precursors was carried out at mild temperatures. Increasing temperature or longer reaction times gave full conversion to the Au(III) carbene complexes **5a–b** previously described by our group.

All the allene-based metal complexes were tested as catalysts in benchmark reactions for Pd (Mizoroki–Heck cross-coupling), Pt and Au (enyne cyclisation and nucleophilic addition to allenes). The symmetric Pd(II) complex **2a** performed well in the Mizoroki–Heck cross coupling of iodobenzene and styrene, giving good yields under standard reaction conditions without the need for additives. All the complexes performed well in the cycloisomerisation reaction of enynes. The Pd(II) and Pt(IV) complexes worked at higher temperatures in the presence of silver salts, while the Au(III) complexes worked at room temperatures. We observed a switch in selectivity towards different isomeric products depending on the metal complex used. The Au(III) complexes **4a–b** were the most active catalysts in alkoxylation reaction of N-tethered enynes, while the Pt(IV) analogues **3a–b** performed well with all type of enynes and best in the nucleophilic addition to allenes to give double addition products. Further studies on the asymmetric version of the ligands and their application in asymmetric catalysis are undergoing in our laboratories.

Finally, studies of the new complexes as new antimicrobial and anticancer agents gave very promising preliminary results. Although Pt(IV) complexes did not show biological activity, possibly due to solubility issues or their difficulty of *in situ* reduction to potentially active Pt(II) derivatives, the Pd(II) and Au(III) analogues showed good activity in both antimicrobial and anticancer assays, as well as interaction with different DNA structures. In particular it is worth highlighting the Pd(II) complex **2a** that showed good activity in the antimicrobial and anticancer assays and an unusual destabilisation of the hTeloC i-motif DNA structure, which is notoriously hard to achieve, and could begin to explain its biological activity. This peculiar interaction with i-motif secondary structures makes this work highly novel and would open new avenues of research in the area of metallodrugs using Pd complexes with alternative biological mechanisms of action.

## Author contributions

H. K. M. contributed to all the experimental work, writing of the original draft of the manuscript, later reviewing, editing and the whole ESL.† C. A. V. contributed to the MDA-MB-231 cell cultures, provided help with the anticancer assays, and reviewing of the manuscript. Y. X. carried out the FID and CD assays. M. J. M. provided training, supervision and analysis of the anticancer assays and contributed to writing, reviewing, and editing the manuscript. Z. A. E. W. provided guidance and analysis of the experiments with DNA, and contributed to writing, reviewing, and editing the manuscript. M. P. M. supervised the entire research with conceptualisation, analysis, and resources,

contributed to the writing, and coordinated the reviewing and editing of the final manuscript.

## Conflicts of interest

There are no conflicts to declare.

## Acknowledgements

The DNA and the anticancer experiments use synthetic DNA sequences and cultured human cell lines that do not have any associated ethic approvals. The antimicrobial work carried out by the CO-ADD was performed in strict accordance with The Australian Code for the Responsible Conduct of Research (2018). Human blood was sourced from the Australian Red Cross Blood Service with informed consent, and its use in haemolysis assays was approved by The University of Queensland Institutional Human Research Ethics Committee, Approval Number 2014000031.

Funding by the Faculty of Science at the University of East Anglia is gratefully acknowledged (H. K. M. and C. A. V.). C. A. V. would like to thank Mr and Mrs Whittaker for her oncology fellowship. Authors would like to thank Dr John Fielden (UEA) for help with the electrochemistry, Dr Rianne Lord (UEA) for her help with the MTT assay, Dr Abdul-Sada (University of Sussex) for HRMS analysis and Stephen Boyer (London Metropolitan University) for elemental analysis. Antimicrobial screening was performed by CO-ADD (Community for Open Antimicrobial Drug Discovery), funded by the Wellcome Trust (UK) and The University of Queensland (Australia).

## Notes and references

- 1 F. Lovering, J. Bikker and C. Humblet, *J. Med. Chem.*, 2009, **52**, 6752–6756.
- 2 A. W. Hung, A. Ramek, Y. Wang, T. Kaya, J. A. Wilson, P. A. Clemons and D. W. Young, *Proc. Natl. Acad. Sci. U. S. A.*, 2011, **108**, 6799–6804.
- 3 F. Lovering, *MedChemComm*, 2013, **4**, 515–519.
- 4 C. H. Arrowsmith, J. E. Audia, C. Austin, J. Baell, J. Bennett, J. Blagg, C. Bountra, P. E. Brennan, P. J. Brown, M. E. Bunnage, C. Buser-Doepner, R. M. Campbell, A. J. Carter, P. Cohen, R. A. Copeland, B. Cravatt, J. L. Dahlin, D. Dhanak, A. M. Edwards, M. Frederiksen, S. V. Frye, N. Gray, C. E. Grimshaw, D. Hepworth, T. Howe, K. V. M. Huber, J. Jin, S. Knapp, J. D. Kotz, R. G. Kruger, D. Lowe, M. M. Mader, B. Marsden, A. Mueller-Fahrnow, S. Müller, R. C. O'Hagan, J. P. Overington, D. R. Owen, S. H. Rosenberg, R. Ross, B. Roth, M. Schapira, S. L. Schreiber, B. Shoichet, M. Sundström, G. Superti-Furga, J. Taunton, L. Toledo-Sherman, C. Walpole, M. A. Walters, T. M. Willson, P. Workman, R. N. Young and W. J. Zuercher, *Nat. Chem. Biol.*, 2015, **11**, 536–541.



- 5 R. H. Holm, P. Kennepohl and E. I. Solomon, *Chem. Rev.*, 1996, **96**, 2239–2314.
- 6 K. D. Mjos and C. Orvig, *Chem. Rev.*, 2014, **114**, 4540–4563.
- 7 C. N. Morrison, K. E. Prosser, R. W. Stokes, A. Cordes, N. Metzler-Nolte and S. M. Cohen, *Chem. Sci.*, 2020, **11**, 1216–1225.
- 8 J.-H. Xie and Q.-L. Zhou, *Acc. Chem. Res.*, 2008, **41**, 581–593.
- 9 W. Sommer and D. Weibel, *Chemfiles*, 2008, **8**, 1–92.
- 10 A. Pfaltz and W. J. Drury III, *Proc. Natl. Acad. Sci. U. S. A.*, 2004, **101**, 5723–5726.
- 11 W. W. Brandt, F. P. Dwyer and E. D. Gyrfas, *Chem. Rev.*, 1954, **54**, 959–1017.
- 12 N. Krause and A. S. K. Hashmi, in *Modern Allene Chemistry*, WILEY-VCH Verlag GmbH & Co. KGaA, Weinheim, 2004, vol. 1, p. 54.
- 13 A. Hoffmann-Röder and N. Krause, *Angew. Chem., Int. Ed.*, 2004, **43**, 1196–1216.
- 14 M. A. Sierra, L. Casarrubios and M. C. de la Torre, *Chem. – Eur. J.*, 2019, **25**, 7232–7242.
- 15 A. Frei, J. Zuegg, A. G. Elliott, M. Baker, S. Braese, C. Brown, F. Chen, C. G. Dowson, G. Dujardin, N. Jung, A. P. King, A. M. Mansour, M. Massi, J. Moat, H. A. Mohamed, A. K. Renfrew, P. J. Rutledge, P. J. Sadler, M. H. Todd, C. E. Willans, J. J. Wilson, M. A. Cooper and M. A. T. Blaskovich, *Chem. Sci.*, 2020, **11**, 2627–2639.
- 16 K. Okamoto, Y. Kai, N. Yasuoka and N. Kasai, *J. Organomet. Chem.*, 1974, **65**, 427–441.
- 17 T. J. Brown, A. Sugie, M. G. Dickens and R. A. Widenhoefer, *Organometallics*, 2010, **29**, 4207–4209.
- 18 M. T. Quirós, M. P. Muñoz, J. Christensen and S. J. Coles, *Organometallics*, 2017, **36**, 318–330.
- 19 A. L. Colebatch, I. A. Cade, A. F. Hill and M. M. Bhadbhade, *Organometallics*, 2013, **32**, 4766–4774.
- 20 For other examples of allene containing phosphines as ligands for metal complexes see: E. V. Banide, J. P. Grealis, H. Müller-Bunz, Y. Ortin, M. Casey, C. Mendicute-Fierro, M. Cristina Lagunas and M. J. McGlinchey, *J. Organomet. Chem.*, 2008, **693**, 1759–1770 and ref. 21. No applications of these phosphine- and phosphine oxide-containing fluorenyl(allene) complexes have been reported.
- 21 S. Milosevic, E. V. Banide, H. Müller-Bunz, D. G. Gilheany and M. J. McGlinchey, *Organometallics*, 2011, **30**, 3804–3817.
- 22 S. Löhr, J. Averbeck, M. Schürmann and N. Krause, *Eur. J. Inorg. Chem.*, 2008, 552–556.
- 23 F. Cai, X. Pu, X. Qi, V. Lynch, A. Radha and J. M. Ready, *J. Am. Chem. Soc.*, 2011, **133**, 18066–18069.
- 24 A. Vanitcha, C. Damelin-court, G. Gontard, N. Vanthuyne, V. Mouriès-Mansuy and L. Fensterbank, *Chem. Commun.*, 2016, **52**, 6785–6788.
- 25 F. Cai, N. D. Thangada, E. Pan and J. M. Ready, *Organometallics*, 2013, **32**, 5619–5622.
- 26 S. Sentets, R. Serres, Y. Ortin, N. Lukan and G. Lavigne, *Organometallics*, 2008, **27**, 2078–2091.
- 27 A. Vanitcha, G. Gontard, N. Vanthuyne, E. Derat, V. Mouriès-Mansuy and L. Fensterbank, *Adv. Synth. Catal.*, 2015, **357**, 2213–2218.
- 28 H. K. Maliszewska, D. L. Hughes and M. P. Muñoz, *Dalton Trans.*, 2020, **49**, 4034–4038.
- 29 A. Fürstner and P. W. Davies, *Angew. Chem., Int. Ed.*, 2007, **46**, 3410–3449.
- 30 E. Jiménez-Núñez and A. M. Echavarren, *Chem. Rev.*, 2008, **108**, 3326–3350.
- 31 S. P. Nolan, *Acc. Chem. Res.*, 2011, **44**, 91–100.
- 32 C. Praveen, *Coord. Chem. Rev.*, 2019, **392**, 1–34.
- 33 B. W. Harper, A. M. Krause-Heuer, M. P. Grant, M. Manohar, K. B. Garbutcheon-Singh and J. R. Aldrich-Wright, *Chem. – Eur. J.*, 2010, **16**, 7064–7077.
- 34 B. Bertrand, M. R. M. Williams and M. Bochmann, *Chem. – Eur. J.*, 2018, **24**, 11840–11851.
- 35 X. Wang, X. Wang, S. Jin, N. Muhammad and Z. Guo, *Chem. Rev.*, 2019, **119**, 1138–1192.
- 36 A. R. Kapdi and I. J. S. Fairlamb, *Chem. Soc. Rev.*, 2014, **43**, 4751–4777.
- 37 N. C. Vieira, J. A. Pienkos, C. D. McMillen, A. R. Myers, A. P. Clay and P. S. Wagenknecht, *Dalton Trans.*, 2017, **46**, 15195–15199.
- 38 L. D. Jaques, S. L. McDarmont, M. M. Smart, C. D. McMillen, S. E. Neglia, J. P. Lee and J. A. Pienkos, *Inorg. Chem. Commun.*, 2020, **112**, 107722–107727.
- 39 T. Kawano, T. Shinomaru and I. Ueda, *Org. Lett.*, 2002, **4**, 2545–2547.
- 40 Interestingly the bis(phosphine)allene-Pd complex reported by Fensterbank (see ref. 27) shows a *cis* arrangement, a bent allene backbone (151.3°) and  $\Delta\delta = 16.6$  ppm of the central allene carbon in <sup>13</sup>C NMR.
- 41 R. D. Shannon, *Acta Crystallogr., Sect. A: Cryst. Phys., Diffraction, Theor. Gen. Crystallogr.*, 1976, **32**, 751–767.
- 42 R. Kuroda, S. Neidle, I. M. Ismail and P. J. Sadler, *Inorg. Chem.*, 1983, **22**, 3620–3624.
- 43 M. D. Hall and T. W. Hambley, *Coord. Chem. Rev.*, 2002, **232**, 49–67.
- 44 Y. Shi, S.-A. Liu, D. J. Kerwood, J. Goodisman and J. C. Dabrowiak, *J. Inorg. Biochem.*, 2012, **107**, 6–14.
- 45 D. Höfer, H. P. Varbanov, M. Hejl, M. A. Jakupec, A. Roller, M. Galanski and B. K. Keppler, *J. Inorg. Biochem.*, 2017, **174**, 119–129.
- 46 I. P. Beletskaya and A. V. Cheprakov, *Chem. Rev.*, 2000, **100**, 3009–3066.
- 47 A. B. Dounay and L. E. Overman, *Chem. Rev.*, 2003, **103**, 2945–2964.
- 48 C. C. C. Johansson Seechurn, M. O. Kitching, T. J. Colacot and V. Snieckus, *Angew. Chem., Int. Ed.*, 2012, **51**, 5062–5085.
- 49 C. Aubert, O. Buisine and M. Malacria, *Chem. Rev.*, 2002, **102**, 813–834.
- 50 L. Fensterbank and M. Malacria, *Acc. Chem. Res.*, 2014, **47**, 953–965.



- 51 M. T. Quirós and M. P. Muñoz, in *Au-Catalyzed Synthesis and Functionalization of Heterocycles*, Springer, Cham, 2016, vol. 46, pp. 117–174.
- 52 C. García-Morales and A. Echavarren, *Synlett*, 2018, 2225–2237.
- 53 D. Wang, R. Cai, S. Sharma, J. Jirak, S. K. Thummanapelli, N. G. Akhmedov, H. Zhang, X. Liu, J. L. Petersen and X. Shi, *J. Am. Chem. Soc.*, 2012, **134**, 9012–9019.
- 54 A. Franchino, M. Montesinos-Magraner and A. M. Echavarren, *Bull. Chem. Soc. Jpn.*, 2021, **94**, 1099–1117.
- 55 M. P. Muñoz, M. Méndez, C. Nevado, D. J. Cárdenas and A. M. Echavarren, *Synthesis*, 2003, 2898–2902.
- 56 L. Charruault, V. Michelet, R. Taras, S. Gladiali and J.-P. Genêt, *Chem. Commun.*, 2004, 850–851.
- 57 C. Nieto-Oberhuber, M. P. Muñoz, S. López, E. Jiménez-Núñez, C. Nevado, E. Herrero-Gómez, M. Raducan and A. M. Echavarren, *Chem. – Eur. J.*, 2006, **12**, 1677–1693.
- 58 N. Krause, Ö. Aksin-Artok, M. Asikainen, V. Breker, C. Deutsch, J. Erdsack, H.-T. Fan, B. Gockel, S. Minkler, M. Poonoth, Y. Sawama, Y. Sawama, T. Sun, F. Volz and C. Winter, *J. Organomet. Chem.*, 2012, **704**, 1–8.
- 59 M. P. Muñoz, *Chem. Soc. Rev.*, 2014, **43**, 3164–3183.
- 60 M. Paz Muñoz, M. C. de la Torre and M. A. Sierra, *Adv. Synth. Catal.*, 2010, **352**, 2189–2194.
- 61 M. P. Muñoz, M. C. de la Torre and M. A. Sierra, *Chem. – Eur. J.*, 2012, **18**, 4499–4504.
- 62 L. Cooper, J. M. Alonso, L. Eagling, H. Newson, S. Herath, C. Thomson, A. Lister, C. Howsham, B. Cox and M. P. Muñoz, *Chem. – Eur. J.*, 2018, **24**, 6105–6114.
- 63 M. T. Quirós, E. Gómez-Bengoia and M. P. Muñoz, *Pure Appl. Chem.*, 2020, **92**, 167–177.
- 64 Menggenbateer, M. Narsireddy, G. Ferrara, N. Nishina, T. Jin and Y. Yamamoto, *Tetrahedron Lett.*, 2010, **51**, 4627–4629.
- 65 M. P. Muñoz, *Org. Biomol. Chem.*, 2012, **10**, 3584–3594.
- 66 R. J. Harris, R. G. Carden, A. N. Duncan and R. A. Widenhoefer, *ACS Catal.*, 2018, **8**, 8941–8952.
- 67 There is one example of the di-Au(i)-mono phosphine complex reported by Fensterbank (see ref. 24) used as catalyst in the cyclisation of allenediene.
- 68 M. A. T. Blaskovich, J. Zuegg, A. G. Elliott and M. A. Cooper, *ACS Infect. Dis.*, 2015, **1**, 285–287.
- 69 MIC is defined as the lowest concentration of the drug at which full inhibition of the bacteria and fungi growth has been detected (inhibition >80%) with the next highest concentration also exhibiting full growth inhibition. The compounds with MIC of 16  $\mu\text{g mL}^{-1}$  or lower were deemed active.
- 70 The lowest MIC value against SA recently reported by CO-ADD was 0.5  $\mu\text{g mL}^{-1}$  for an Ir complex. A Ru complex gave the lowest MIC value against Ca, 0.125  $\mu\text{g mL}^{-1}$ . Few complexes were reported for activity against Cn, and a different Ir complex showed the lowest MIC value of 0.5  $\mu\text{g mL}^{-1}$ . See ref. 15.
- 71 Previously reported antimicrobial activity of Pd complexes was lower (MIC > 100  $\mu\text{g mL}^{-1}$  in G. Onar, C. Güsters, M. O. Karatas, S. Balcioglu, N. Akbay, N. Özdemir, B. Ates and B. Alici, *J. Organomet. Chem.*, 2019, **886**, 48–56; and MICs = 0.0197–5.0  $\text{mg mL}^{-1}$  for bacteria in S. Y. Hussaini, R. A. Haque and M. R. Razali, *J. Organomet. Chem.*, 2019, **882**, 96–111).
- 72 The haemolytic activity against human red blood cells (RBC) was determined as a HC<sub>10</sub> value – concentration at 10% haemolytic activity (Table 4). Values with the “>” sign indicate a sample with no haemolytic activity or samples with HC<sub>10</sub> values above the maximum tested concentration.
- 73 M. Patra, G. Gasser and N. Metzler-Nolte, *Dalton Trans.*, 2012, **41**, 6350–6358.
- 74 B. D. Glišić and M. I. Djuran, *Dalton Trans.*, 2014, **43**, 5950–5969.
- 75 A. Frei, *Antibiotics*, 2020, **9**, 90–114.
- 76 B. Bertrand and A. Casini, *Dalton Trans.*, 2014, **43**, 4209–4219.
- 77 A. M. Mansour and O. R. Shehab, *Eur. J. Inorg. Chem.*, 2019, 2830–2838.
- 78 R. K. Mahato, A. K. Mahanty, S. Paul, V. Gopal, B. Perumalsamy, G. Balakrishnan, T. Ramasamy, D. Dharumadurai and B. Biswas, *J. Mol. Struct.*, 2021, **1223**, 129264–129274.
- 79 P. Chakraborty, D. Oosterhuis, R. Bonsignore, A. Casini, P. Olinga and D.-J. Scheffers, *ChemMedChem*, 2021, **16**, 3060–3070.
- 80 K. J. Chavez, S. V. Garimella and S. Lipkowitz, *Breast Dis.*, 2010, **32**, 35–48.
- 81 E. Ulukaya, F. Ari, K. Dimas, E. I. Ikitimur, E. Guney and V. T. Yilmaz, *Eur. J. Med. Chem.*, 2011, **46**, 4957–4963.
- 82 F. Ari, E. Ulukaya, M. Sarimahmut and V. T. Yilmaz, *Bioorg. Med. Chem.*, 2013, **21**, 3016–3021.
- 83 J. Haribabu, S. Srividya, D. Mahendiran, D. Gayathri, V. Venkatramu, N. Bhuvanesh and R. Karvembu, *Inorg. Chem.*, 2020, **59**, 17109–17122.
- 84 Z. Zhang, G. Du, G. Gong, Y. Sheng, X. Lu, W. Cai, F. Wang and G. Zhao, *J. Mol. Struct.*, 2021, **1232**, 130021–130027.
- 85 S. Kimani, S. Chakraborty, I. Irene, J. de la Mare, A. Edkins, A. du Toit, B. Loos, A. Blanckenberg, A. Van Niekerk, L. V. Costa-Lotufo, K. Aruljothi, S. Mapolie and S. Prince, *Biochem. Pharmacol.*, 2021, **190**, 114598–114615.
- 86 M. Williams, A. I. Green, J. Fernandez-Cestau, D. L. Hughes, M. A. O’Connell, M. Searcey, B. Bertrand and M. Bochmann, *Dalton Trans.*, 2017, **46**, 13397–13408.
- 87 S. Montanel-Pérez, R. Elizalde, A. Laguna, M. D. Villacampa and M. C. Gimeno, *Eur. J. Inorg. Chem.*, 2019, 4273–4281.
- 88 S. M. Cohen and S. J. Lippard, in *Progress in Nucleic Acid Research and Molecular Biology*, Academic Press, 2001, vol. 67, pp. 93–130.
- 89 C. K. Mirabelli, C.-M. Sung, J. P. Zimmerman, D. T. Hill, S. Mong and S. T. Crooke, *Biochem. Pharmacol.*, 1986, **35**, 1427–1433.



- 90 C. P. Saris, P. M. van de Vaart, R. C. Rietbroek and F. Bloramaert, *Carcinogenesis*, 1996, **17**, 2763–2769.
- 91 L. Messori, P. Orioli, C. Tempi and G. Marcon, *Biochem. Biophys. Res. Commun.*, 2001, **281**, 352–360.
- 92 S. G. Chaney, S. L. Campbell, B. Temple, E. Bassett, Y. Wu and M. Faldu, *J. Inorg. Biochem.*, 2004, **98**, 1551–1559.
- 93 S. Balasubramanian, L. H. Hurley and S. Neidle, *Nat. Rev. Drug Discovery*, 2011, **10**, 261–275.
- 94 E. P. Wright, J. L. Huppert and Z. A. E. Waller, *Nucleic Acids Res.*, 2017, **45**, 13095–13096.
- 95 A. T. Phan, *Nucleic Acids Res.*, 2002, **30**, 4618–4625.
- 96 W. Lu, Y. Zhang, D. Liu, Z. Songyang and M. Wan, *Exp. Cell Res.*, 2013, **319**, 133–141.
- 97 J. W. Shay and S. Bacchetti, *Eur. J. Cancer*, 1997, **33**, 787–791.
- 98 J. A. Brazier, A. Shah and G. D. Brown, *Chem. Commun.*, 2012, **48**, 10739–10741.
- 99 Q. Sheng, J. C. Neaverson, T. Mahmoud, C. E. M. Stevenson, S. E. Matthews and Z. A. E. Waller, *Org. Biomol. Chem.*, 2017, **15**, 5669–5673.
- 100 For an example of anticancer Pt(II) and Au(III) complexes with DNA interactions, see: J. J. Criado, J. L. Manzano and E. Rodríguez-Fernández, *J. Inorg. Chem.*, 2003, **96**, 311–320.
- 101 A. Casini, C. Hartinger, C. Gabbiani, E. Mini, P. J. Dyson, B. K. Keppler and L. Messori, *J. Inorg. Chem.*, 2008, **102**, 564–575.
- 102 A. Bindoli, M. P. Rigobello, G. Scutari, C. Gabbiani, A. Casini and L. Messori, *Coord. Chem. Rev.*, 2009, **253**, 1692–1707.
- 103 V. Milacic and Q. P. Dou, *Chem. Rev.*, 2009, **253**, 1649–1660.
- 104 E. Meggers, *Chem. Commun.*, 2009, 1001–1010.
- 105 A. Casini and L. Messori, *Curr. Top. Med. Chem.*, 2011, **11**, 2647–2660.
- 106 M. Dörr and E. Meggers, *Curr. Opin. Chem. Biol.*, 2014, **19**, 76–81.
- 107 M. Vorlíčková, I. Kejnovská, K. Bednářová, D. Renčíuk and J. Kypr, *Chirality*, 2012, **24**, 691–698.
- 108 E. Gao, M. Zhu, L. Liu, Y. Huang, L. Wang, C. Shi, W. Zhang and Y. Sun, *Inorg. Chem.*, 2010, **49**, 3261–3270.
- 109 M. A. Bork, C. G. Gianopoulos, H. Zhang, P. E. Fanwick, J. H. Choi and D. R. McMillin, *Biochemistry*, 2014, **53**, 714–724.
- 110 G. Onar, C. Gürses, M. O. Karataş, S. Balcioğlu, N. Akbay, N. Özdemir, B. Ateş and B. Alici, *J. Organomet. Chem.*, 2019, **886**, 48–56.
- 111 A. Ali, M. Kamra, S. Roy, K. Muniyappa and S. Bhattacharya, *Bioconjugate Chem.*, 2017, **28**, 341–352.
- 112 We did not observe precipitation in these experiments. Partial precipitation causes scattering at 320 nm, which was not observed.
- 113 A. Pagano, N. Iaccarino, M. A. S. Abdelhamid, D. Brancaccio, E. U. Garzarella, A. Di Porzio, E. Novellino, Z. A. E. Waller, B. Pagano, J. Amato and A. Randazzo, *Front. Chem.*, 2018, **6**, 281–294.
- 114 M. A. S. Abdelhamid, A. J. Gates and Z. A. E. Waller, *Biochemistry*, 2019, **58**, 245–249.

